DFT study of the mechanism and stereoselectivity of the 1,3-dipolar cycloaddition between pyrroline-1-oxide and methyl crotonate

ARTICLE *in* JOURNAL OF CHEMICAL SCIENCES · JANUARY 2014

Impact Factor: 1.19 · DOI: 10.1007/s12039-013-0563-y

4 AUTHORS, INCLUDING:

Najia Komiha
Mohammed V University of Rabat
53 PUBLICATIONS **275** CITATIONS

SEE PROFILE

J. Chem. Sci. Vol. 126, No. 1, January 2014, pp. 283–292.

DFT study of the mechanism and stereoselectivity of the 1,3-dipolar cycloaddition between pyrroline-1-oxide and methyl crotonate

KHADIJA MARAKCHI[a,*], RACHIDA GHAILANE[b], OUM KALTOUM KABBAJ[a] and NAJIA KOMIHA[a]

[a]Laboratoire de Spectroscopie, Modélisation Moléculaire, Matériaux et Environnement (LS3ME) Université Mohammed V-Agdal Faculté des Sciences, BP 1014 Rabat, Maroc

[b]Laboratoire de Synthèse Organique, Organométallique et Théorique. Faculté des Sciences, Université Ibn Tofail, BP 13314 Kénitra, Maroc

e-mail: marakchi_k@yahoo.fr

MS received 22 May 2013; revised 8 October 2013; accepted 23 October 2013

Abstract. A theoretical study of the regio- and stereoselectivities of the 1,3-dipolar cycloaddition reaction between methyl crotonate and pyrroline-1-oxide has been carried out using density functional theory (DFT) at the B3LYP/6-31G(d) level of theory. The reaction has been followed by performing transition state optimization, calculations of intrinsic reaction coordinate and activation energies; the molecular mechanism of the reactions is concerted and asynchronous. The regio- and exo/endo-selectivity have been explained in terms of frontier molecular orbital interactions, local and global electrophilicity and nucleophilicity indices and an analysis of the Wiberg bond indices in the transition state. The FMO analysis and DFT-based reactivity indices showed that the regioselectivity of this reaction is controlled by the $HOMO_{dipole}$–$LUMO_{dipolarophile}$ interaction. The activation parameters indicated favoured endo approach along the meta-pathway in agreement with the experimental results.

Keywords. Pyrroline-1-oxide; dipolar cycloaddition; optimized structures; stereoselectivity; DFT-based reactivity indices.

1. Introduction

1,3-Dipolar cycloaddition (1,3-DC) is one of the simplest approaches for the construction of five-membered heterocyclic rings.[1] Reactions between nitrones and alkenes leading to isoxazolidines are well-known construction processes.[1,2] Substituted isoxazolidines are interesting biological active compounds[3] and could be used as enzyme inhibitors.[4,5] They are also frequently used as intermediates for the synthesis of a variety of compounds after cleavage of the N–O bond.[6]

In the context of the cycloadditions of nitrones with several dipolarophiles, we have reported a density functional theory (DFT) study of 1,3-dipolar cycloaddition reaction between simple nitrone with three-fluorinated dipolarophiles, analysis of the results on different reaction pathways shows that the reaction occurs through a concerted process and proceed more or less synchronously.[7] We have also studied the molecular mechanism for the 1,3-dipolar cycloaddition of nitrone with sulphonylethene chloride using *ab initio* and DFT methods at the HF, MP2 and B3LYP levels together with the 6-31G* basis set. Activation energies and asynchronicity are dependent on the computation level. Thus, while HF calculations gave large barriers, MP2 calculations tend to underestimate them. DFT calculations gave reasonable values.[8] Liu *et al.*[9] have performed DFT calculations at B3LYP/6-31G* level on the 1,3-dipolar cycloaddition reaction of the simplest nitrone to dipolarophiles containing electron-releasing substituents. Here, the endo approach is kinetically favoured because of stabilization of the secondary orbital interactions. In another study, Cossó *et al.*[10] have used B3LYP/6-31G* calculations to study the 1,3-dipolar cycloaddition reaction of unsubstituted nitrone with nitroethene. Asynchronicity in the bond formation process in the two regioisomeric approaches of the two reactants is found to be controlled by the electron-deficient dipolarophile. Domingo *et al.* have studied the 1,3-dipolar cycloaddition reaction of nitrones with several dipolarophiles using DFT methods at the B3LYP/6-31G* and B3LYP/6-31+G* levels.[11,12] Their calculations predict an asynchronous concerted mechanism and both stereo and regioselectivity were found dependent on the computational model and computational level. Nacereddine *et al.*[13]

*For correspondence

have studied the regio- and stereoselectivities of the 1,3-dipolar cycloaddition of C-diethoxyphosphoryl-N-methylnitrone with substituted alkenes (allyl alcohol and methyl acrylate) using DFT method. An analysis of potential energy surfaces (PESs) shows that these 1,3-dipolar cycloaddition reactions favour the formation of the ortho-trans cycloadduct in agreement with experimental data. Stecko *et al.* have reported a DFT/B3LYP/6-31+G(d) study of the 1,3-dipolar cycloaddition of cyclic nitrones with electron-poor and electron-rich cyclic dipolarophiles: α, β-unsaturated lactones and vinyl ethers. Different reaction channels and reactants approaches, effective in regio- and stereochemical preferences are discussed; the results were compared to experimental data and found in good agreement.[14] Recently, Acharjee and Banerji[15] studied the 1,3-dipolar cycloaddition between C,N-diphenyl nitrone and an unsymmetrical disubstituted olefin at DFT/B3LYP/6-31G(d) level of theory. The analysis of FMO energies, reactivity indices and charge transfer in the transition states indicates a normal electron demand character for the reaction.

The experimental investigations of Asrof *et al.*[16] implied that the cycloaddition between pyrroline-1-oxide **1** to dipolarophile **3b** (methyl crotonate) gives a mixture of substituted isoxazolidines **4b** and **5b** in a 93:7 ratio, respectively (scheme 1). In what follows, we present a DFT study on the cycloaddition reaction involving cyclic 5-membered nitrone with methyl crotonate. Our results are presented and discussed on the basis of the generated trends in terms of detailed conceptual DFT-based reactivity indices and the analysis of stationary points on the potential energy surfaces. This analysis allows to elucidate the regio- and stereoselectivities of the 1,3-dipolar cycloaddition and to explain the experimental observations.

2. Computational details

All calculations reported in this paper were performed using Gaussian 03 suite of programs[17] along with the graphical interface GaussView3.08. The full geometrical optimization of all structures and transition states structures (TSs) were carried out with DFT by applying the Becke's[18] three-parameter hybrid functional and Lee-Yang-Parr's[19] correlation functional. The basis set 6-31G(d)[20] has been employed for the prediction of activation energies of cycloaddition reactions and to provide geometries and electronic properties. The stationary points were characterized by frequency calculations in order to check that the TSs had one and only one imaginary frequency with the corresponding eigenvector involving the formation of the newly created C–C and C–O bonds. Furthermore, the intrinsic reaction coordinate (IRC)[21,22] path was mapped to authenticate the connection of a TS to the two associated minima of the proposed mechanism. Electronic structures of critical points were analysed by the natural bond orbital (NBO) method.[23] Global reactivity indices were estimated according to the equations recommended by Parr and Yang.[24] In particular, the electronic chemical potentials (μ) and chemical hardness (η) of the reactants studied were evaluated in terms of the one-electron energies of the frontier molecular orbital HOMO and LUMO, using the following equations:

$$\mu = (E_{\mathrm{HOMO}} + E_{\mathrm{LUMO}})/2, \tag{1}$$

$$\eta = E_{\mathrm{LUMO}} - E_{\mathrm{HOMO}}. \tag{2}$$

The values of μ and η were then used for the calculation of global electrophilicity (ω) according to the formula:

$$\omega = \mu^2/2\eta. \tag{3}$$

The global nucleophilicity (N)[25] is referred to tetracyanoethylene (TCE) because it presents the lowest HOMO energy and a very large electrophilicity (ω = 5.95 eV) in a large series of molecules already investigated in the context of polar cycloadditions. The global nucleophilicity can then be expressed as:

$$N = E_{\mathrm{HOMO(nucleophile)}} - E_{\mathrm{HOMO(TCE)}}. \tag{4}$$

The local electrophilicity (ω_k)[26] condensed to atom k was calculated by projecting the indice ω onto any

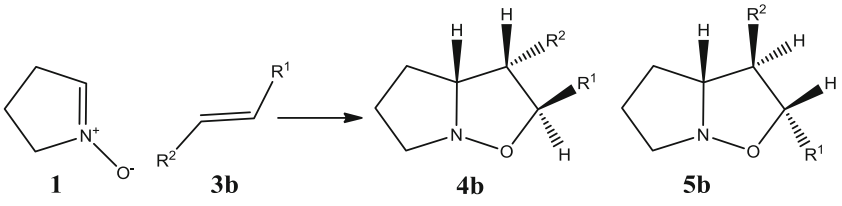

Scheme 1. 1,3-Dipolar cycloaddition of pyrroline-1-oxide with methylcrotonate.

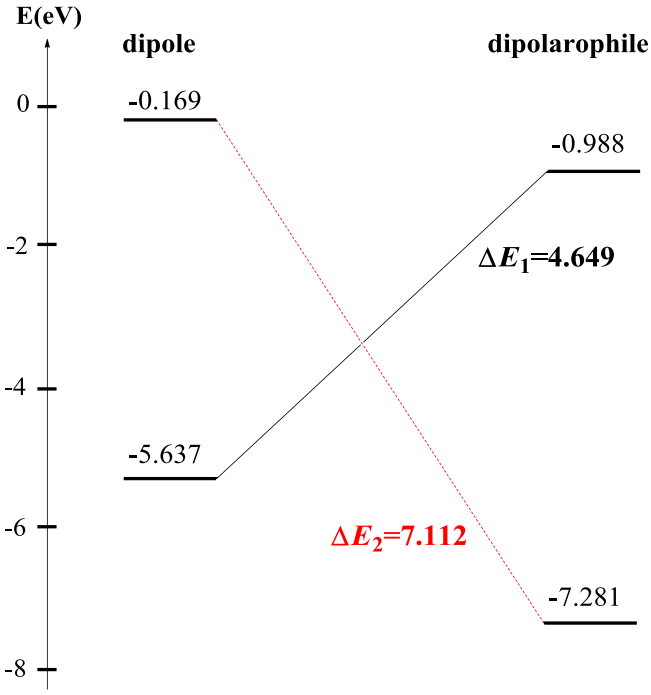

Figure 1. Frontier molecular orbital (B3LYP/6-31G*)) interaction in the 1,3-DC between pyrroline-1-oxide and methyl crotonate.

reaction centre k of the molecule by using Fukui function f_k^+.[27]

$$\omega_k = \omega\, f_k^+. \tag{5}$$

The local nucleophilicity (N_k)[28] condensed to atom k was calculated using global nucleophilicity N and Fukui function f_k^- according to the formula:

$$N_k = N f_k^-. \tag{6}$$

For an atom k in a molecule, depending upon the type of electron transfer, we have three different types of condensed Fukui function defined as follows.[29]

$$f_k^+ = \rho_k\,(N+1) - \rho_k\,(N) \quad \text{(for nucleophilic attack)}, \tag{7}$$

$$f_k^- = \rho_k\,(N) - \rho_k\,(N-1) \quad \text{(for electrophilic attack)}, \tag{8}$$

$$f_k^0 = \frac{\rho_k\,(N+1) - \rho_k\,(N-1)}{2} \quad \text{(for radical attack)}, \tag{9}$$

where $\rho_k(N+1)$, $\rho_k(N)$ and $\rho_k(N-1)$ are defined as the grosselectronic populations of the site k in the anionic, neutral and cationic species, respectively.

3. Results and discussions

For this 1,3-DC reaction between cyclic nitrone: pyrroline-1-oxide and methyl crotonate, we first evaluated the geometrical parameters and energies of all the stationary points (reactants, transition structures and cycloadducts) at DFT/B3LYP/6-31G(d). Population analysis at the transition structures in terms of bond orders and natural charges was performed, together with an analysis based on the global and local reactivity indices of the reactants involved during the cycloadditions.

3.1 *Regiochemistry of 1,3-dipolar cycloaddition reaction based on FMOs and reactivity indices analysis*

3.1a *FMOs analysis*: In this section, the frontier molecular orbital theory[30–39] was applied to explain the regioselectivity and reactivity in 1,3-dipolar cycloaddition of methyl crotonate and the nitrone.

Analysis of the frontier molecular orbitals of the reactants show that in the nitrone, both HOMO and LUMO are π molecular orbitals (MOs). However, in the methyl crotonate, the HOMO is a nonbonding MO localized essentially on the oxygen of the carbonyl group and, in consequence, it is expected that it will not be directly involved in the 1,3-DC process. The HOMO-1 of dipolarophile is a bonding π molecular orbital with a large contribution of the atoms present at the active sites, thus the relative reactivity can be explained with analysis of this MO.

For a better visualization of the FMO approach, we have presented in figure 1 the two possible interactions: $\text{HOMO}_{\text{dipole}}$–$\text{LUMO}_{\text{dipolarophile}}$ ($\Delta E_1 = 4.649$ eV) and $(\text{HOMO-1})_{\text{dipolarophile}}$–$\text{LUMO}_{\text{dipole}}$ (ΔE_2=7.112eV). The FMO analysis for this cycloaddition shows that the main interactions occur between the HOMO dipole and the LUMO dipolarophile, thereby revealing normal electronic demand character of the cycloaddition reaction. This agrees with Sustmann's type

Table 1. Molecular coefficients of the frontier molecular orbitals of the dipole and dipolarophile systems.

Dipole				Dipolarophile			
HOMO		LUMO		HOMO-1		LUMO	
O_1	C_3	O_1	C_3	C_4	C_5	C_4	C_5
0.4793	−0.3793	0.3024	0.4001	0.3522	0.3882	0.3976	−0.2472

Table 2. HOMO, LUMO energies (in a.u.), electronic chemical potential (μ, in a.u.), chemical hardness (η, in a.u.), global electrophilicity (ω, in eV) and global nucleophilicity (N, in eV) for the two reactants.

Reactant	HOMO	LUMO	μ	η	ω	N[a]
Dipole	−0.20715	−0.00622	−0.106685	0.20093	0.770	3.484
dipolarophile[b]	−0.26757	−0.03632	−0.15195	0.23125	1.358	1.840

[a]HOMO energy of tetracyanoethylene is −0.335179 a.u. at the same level of theory
[b]Chemical potential, hardness, electrophilicity and nucleophilicity values are associated to the HOMO-1 of dipolarophile

I reactions.[40,41] According to Houk's rule[42] in general, regioselectivity of of these cycloadditions can be rationalized in terms of more favourable FMO interactions between the largest coefficient centres of the dipole and the dipolarophile. Table 1 shows that the larger orbital coefficients for the binding atoms are that of C_4 of the dipolarophile and O_1 of the dipole, indicating that the important orbital overlap should be between these two atoms. The oxygen of dipole favours an interaction with C_4 of dipolarophile and carbon of dipole interacts with C_5 of dipolarophile to give the meta-regioisomer, which is the major product, obtained experimentally.[16] This result agrees with the 1,3-DC of the cyclic nitrone to methyl propiolate studied by Marco and Domingo[11] who predicted the experimentally observed meta-regioselectivity.

3.1b *Analysis in terms of global and local reactivity of the reactants*: The energies of frontier molecular orbitals, electronic chemical potential (μ), chemical hardness (η), global electrophilicity (ω) and global nucleophilicity (N) for the two reactants have been calculated using equations (1)–(4) and are reported in table 2.

In section 3.1a, we saw that for the dipolarophile, the HOMO cannot be used for interpreting the 1,3-DC, in this case, the chemical potential, hardness, nucleophilicity and electrophilicity have been evaluated using this HOMO-1 and the LUMO energy values.

Electronic chemical potential of pyrroline-1-oxide (−0.106685 a.u.) is higher than that of dipolarophile methyl crotonate (−0.15195 a.u.), indicating thereby that in this 1,3-dipolar cycloaddition, the charge transfer will take place from the dipole to the dipolarophile in agreement with the FMO energy predictions. Values of global electrophilicity of reactants are 1.358 and 0.770 eV, respectively, for methyl crotonate and nitrone. Thus, nitrone **1** will act as a nucleophile whereas alkene **3b** will act as an electrophile, and therefore indicate that the electronic flux is from the dipole to the dipolarophile. The global electrophilicity difference $\Delta\omega$ (0.588 eV) is characteristic of pericyclic reactions,[43,44] which indicates a lower polar character for this cycloaddition. This is also revealed by the low charge transfer observed along this cycloaddition reaction (see section 3.2d). Several studies related to cycloaddition reactions have shown that analysis of the local electrophilicity indice, ω_K at the electrophilic reagent and the nucleophilic indice N_K at the nucleophilic compound explain the observed regioselectivity.[45] Values of the Fukui indices f_k, local and global electrophilicity indices ω_K are reported in table 3 and for better visualization, we have depicted the most favourable two-centre interaction in figure 2. Dipolarophile methyl crotonate has the largest electrophilic activation at the C_4 carbon atom, $\omega_K = 0.340$eV, whereas the dipole pyrroline-1-oxide has the largest nucleophilic activation at the O_1 oxygen atom $N_K = 1.428$ eV. Therefore, C_4 atom of the dipolarophile will be the preferred position for a nucleophilic attack by O_1 of the dipole, leading to the formation of the meta-regioisomer which is in good agreement with the experimental data.[16]

Table 3. Pertinent natural populations and local properties (eV) of pyrroline-1-oxide and methyl crotonate calculated at B3LYP/6-31G(d).

Reactant	site	$\rho(N)$	$\rho(N+1)$	$\rho(N-1)$	f_k^+	f_k^-	ω_k	N_k
Dipole	O_1	−0.50908	−0.714	−0.099	0.205	0.410	0.158	1.428
	C_3	−0.03563	−0.353	0.290	0.317	0.326	0.244	1.135
Dipolarophile[a]	C_4	−0.13191	−0.382	0.088	0.250	0.220	0.340[a]	0.405[a]
	C_5	−0.34803	−0.447	−0.046	0.099	0.302	0.134[a]	0.556[a]

[a]Values in this row were computed with the HOMO-1 contributions (see the text for details)

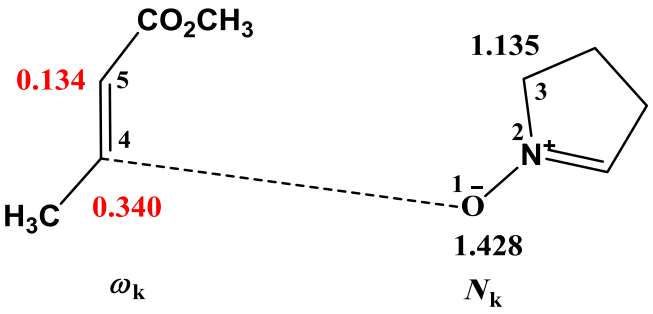

Figure 2. Prediction of favoured interactions between dipole and dipolarophile using DFT-based indices.

This fact agrees with the asynchronicity observed at the transition states (see section 3.2b). The O_1-C_4 or C_3-C_4 bonds formed at the meta-TSs or ortho-TSs are shorter and more advanced than the C_3-C_5 or O_1-C_5 bonds. This is in agreement with other DFT cycloaddition studies[45h] suggesting that the most electrophilic reagents control the asynchronicity of the process by a larger bond-formation process at the most electrophilic site of the molecule.

3.2 *Mechanistic study of the cycloaddition reaction based on activation energy along the different paths of the reaction*

3.2a *Energies of the transition structures*: In the present study, the structures of transition states are located through vibrational frequency analysis. Each transition state is characterized by a single imaginary frequency. We have considered four reactive channels corresponding to the endo and exo-approaches of the dipolarophile towards the dipole via two regioisomeric pathways – ortho and meta. A convenient naming system has been employed for the structures of the transition states and the cycloadducts (scheme 2). So, **TS-oen** and **TS-oex** are the transition structures for the endo and exo approaches of the dipolarophile on the dipole, respectively, along the ortho-channels leading to products, **P-oen** and **P-oex**. Similarly, **TS-men** and **TS-mex** are the TSs for the endo and exo approaches of the dipolarophile on the nitrone, respectively, along the meta-channels leading to products, **P-men** and **P-mex**. The ortho-pathways correspond to the O_1/dipole–C_5/dipolarophile and C_3/dipole–C_4/dipolarophile bond-formation process (5-substituted-CO_2Me-isoxazolidine), whereas the meta-channels correspond to the formation of the 4-substituted-CO_2Me-isoxazolidine by the formation of the O_1/dipole–C_4/dipolarophile and C_3/dipole–C_5/dipolarophile bonds. A schematic representation of the four optimized transition state structures is presented with the atom numbering in figure 3. Total energies (in a.u.) for the all species and relative energies (in kcal/mol) for the TSs and cycloadducts are summarized in table 4. The PESs, corresponding to all the reaction channels, are illustrated in figure 4.

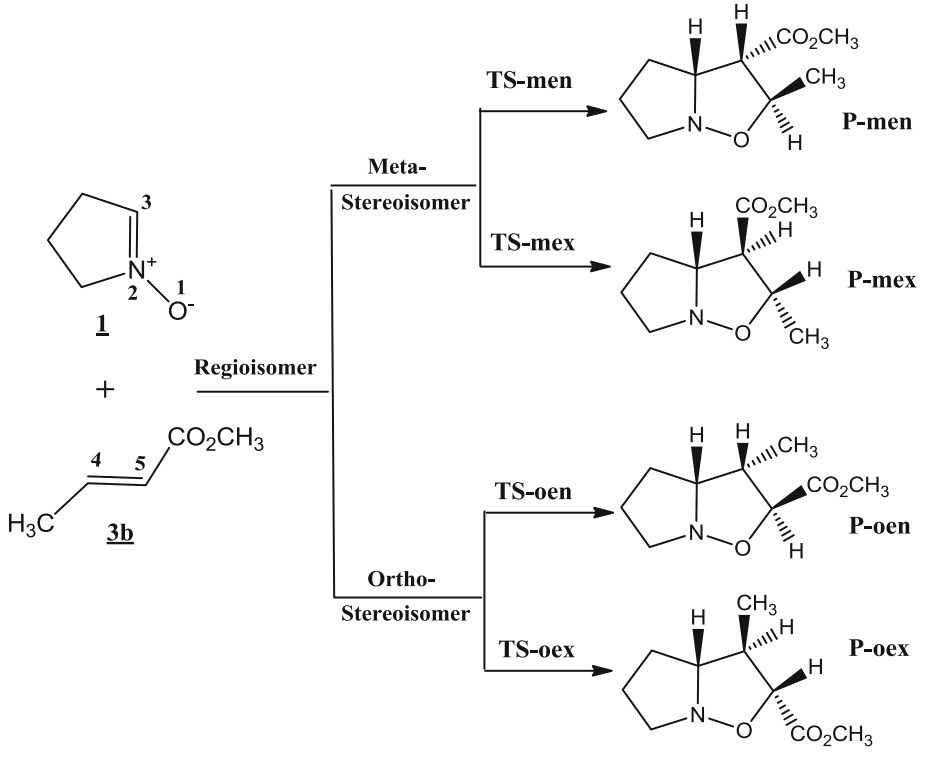

Scheme 2. The exo and endo approaches of pyrroline-1-oxide to alkene **3b**.

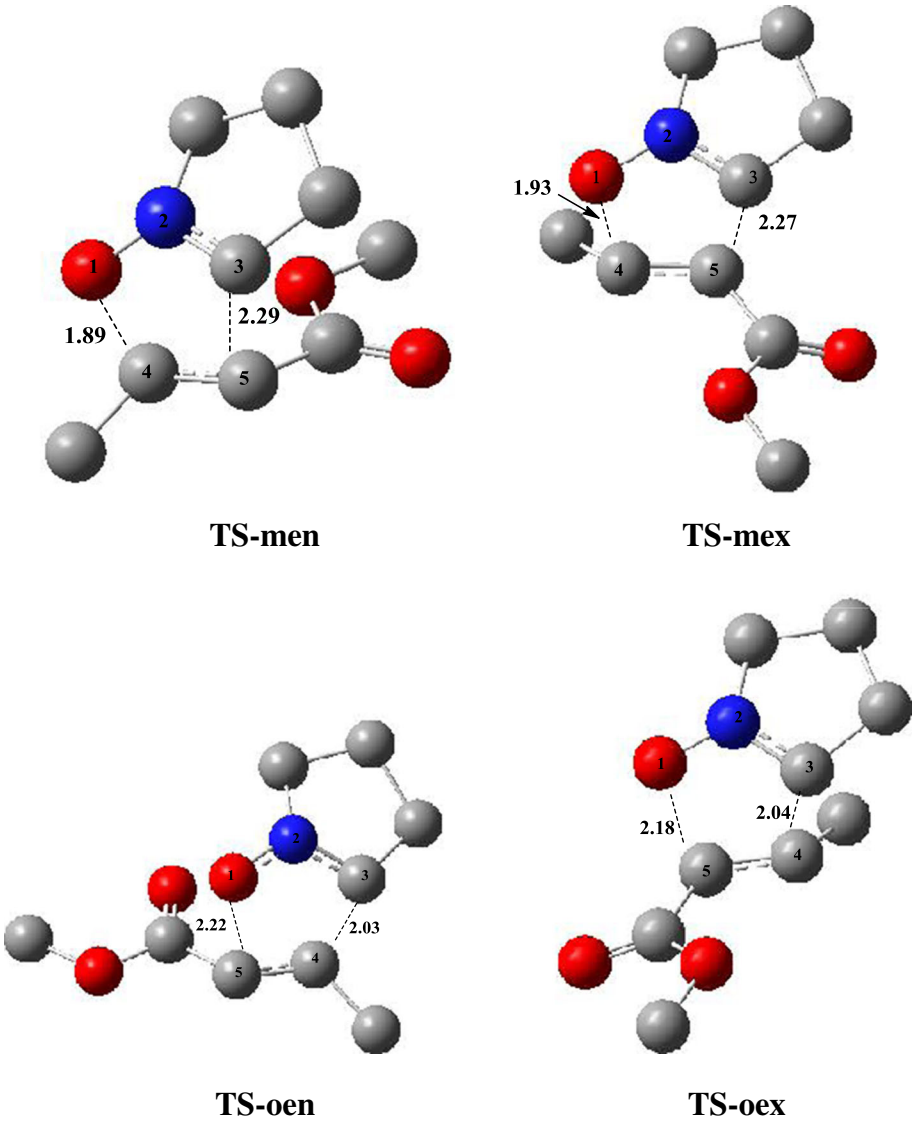

Figure 3. Transition structures corresponding to the regioisomeric path of the 1,3-DC reaction between pyrroline-1-oxide and methyl crotonate. Distances directly involved in the forming-bond process are given in angstroms.

As shown in table 4, the activation barriers associated with the cycloaddition reactions are: 10.4 kcal/mol (**TS-men**), 12.54 kcal/mol (**TS-mex**), 12.77 kcal/mol (**TS-oen**) and 14.84 kcal/mol (**TS-oex**). Accordingly, it can be predicted that the meta/endo-regioisomer will be formed preferentially. Formation of the four cycloadducts **P-men**, **P-mex**, **P-oen** and **P-oex** are exothermic by −18.79, −12.54, −10.08 and −8.83 kcal/mol, respectively. These values reveal that meta-approaches are favoured in regard to ortho ones along the cycloaddition process, in agreement with the FMO analysis. In this case, the kinetic and thermodynamic products are coincident and then only the formation of **P-men** is noticeable, in good agreement with the experimental observations.[16] The favoured formation of the endo-cycloadduct can be attributed to the stabilizing secondary orbital interactions of the ester carbonyl group in the LUMO of the dipolarophile with the HOMO lobe on the nitrogen atom of the cyclic nitrone. This fact is also in agreement with the study of Houk *et al.*[9] who have performed an *ab initio* study on the 1,3-DC of a simple nitrone to dipolarophiles containing electron-releasing substituent. Once again, the endo-cycloadduct was kinetically favoured owing to stabilizing secondary orbital interactions. To take into account the solvent effects, single-point calculations at the B3LYP/6-31G* gas phase optimized geometries have been performed. A self-consistent reaction field (SCRF)[30,46] model based on the polarizable continuum model (PCM) of Tomasi's group[47] have been applied. The solvent used in the experimental study is dichloromethane, so we have used the dielectric

Table 4. Total energies (a.u.) in gas and solvent phases of reactants, transition states and cycloadducts of the 1,3-DC reaction between pyrroline-1-oxide and methyl crotonate and relative energies (kcal/mol).

Stationary point	Gas phase		Dichloromethane solvent	
	E_T	ΔE^*	E_T	ΔE^*
Dipole	−286.5409594		−286.5513743	
Dipolarophile	−345.7883925		−345.7947538	
TS-men	−632.31335235	10.04	−632.3235962	14.14
TS-mex	−632.30937005	12.54	−632.3202759	16.22
P-men	−632.3592947	−18.79	−632.3672016	−13.22
P-mex	−632.34933701	−12.54	−632.3564185	−6.45
TS-oex	−632.30900781	12.77	−632.3169918	18.28
TS-oen	−632.30569459	14.84	−632.3150561	19.49
P-oen	−632.34541471	−10.08	−632.3549487	−5.53
P-oex	−632.34341574	−8.83	−632.3520319	−3.71

* (Reference: Sum of the energies of the reactants)

constant, at 298 K, $\varepsilon = 8.93$. In dichloromethane solvent, the reactants are more stabilized than TSs and cycloadducts. As a consequence, the activation barriers associated with the four TSs: **TS-men**, **TS-mex**, **TS-oen** and **TS-oex** increase to 14.14, 16.22, 18.28 and 19.49 kcal/mol, respectively. Solvent effects decreased the exothermicity of the process because of the greater solvation of the polar nitrone than that of the TSs and cycloadducts.[10,48] We can conclude that the solvent effect produces minor changes of regio and stereoselectivity relative to the gas-phase since the trends of the relatives energies are the same.

3.2b *Geometries of the transition structures*: The optimized geometries of four TSs corresponding to the reaction of pyrroline-1-oxide and methyl crotonate are depicted in figure 3. The corresponding selected geometric parameters, illustrated in table 5, reveal that all transition structures are asynchronous. For both transition structures **TS-men** and **TS-mex**, the Lengths of

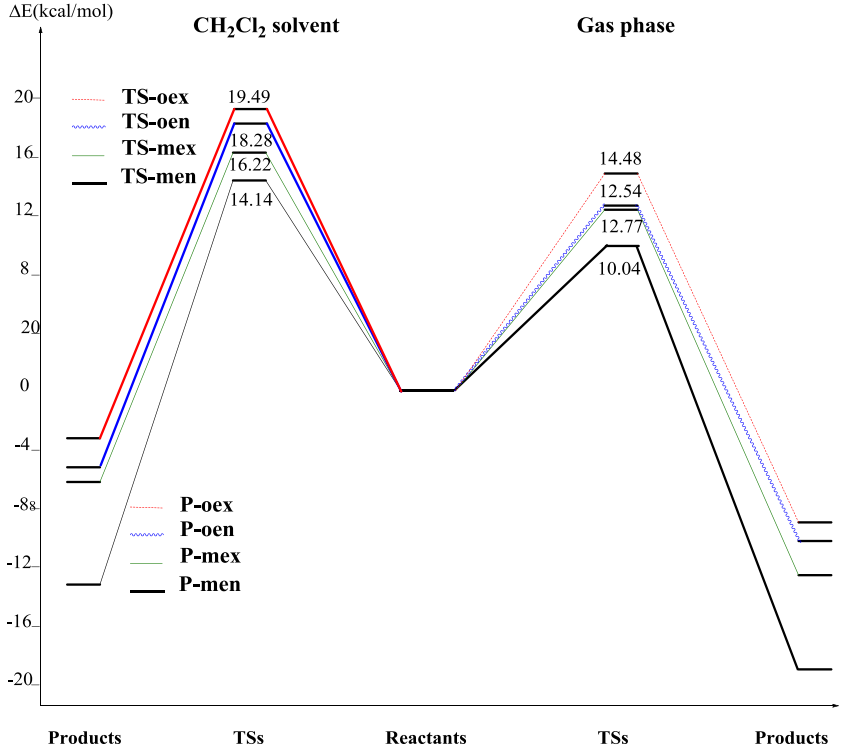

Figure 4. Relative energy profiles (to reactants, in kcal/mol) of stationary points in gas and solvent phases.

Table 5. Bond distances and bond differences (in Angstrom) of the two newly formed bonds at the transition structures.

	Meta-channels				Ortho-channels		
	$d(O_1–C_4)$	$d(C_3–C_5)$	Δd		$d(O_1–C_5)$	$d(C_3–C_4)$	Δd
TS-men	1.89	2.29	0.40	**TS-oen**	2.22	2.03	0.18
TS-mex	1.93	2.27	0.34	**TS-oex**	2.18	2.04	0.14

the C–C forming bonds (2.29 and 2.27 Å) are markedly longer than that of the C–O forming bonds (1.89 and 1.93 Å) showing a significantly dissymmetry for the two newly formed bonds in these TSs. However, in the ortho-pathways, C–O forming bond in **TS-oen** and **TS-oex** (2.18 and 2.22 Å) is longer than C–C forming bonds (2.04 and 2.03 Å). This shows a change of the asynchronicity on the bond formation process for the two regioisomeric pathways. The degree of asynchronicity, Δd, can be determined by considering the difference between the lengths of the two forming bonds such that $\Delta d = |d(C–O) - d(C–C)|$ as shown in table 5. It appears clearly that the meta-TSs are more asynchronous ($\Delta d \approx 0.34–0.40$ Å) than the ortho ones ($\Delta d \approx 0.14–0.18$ Å). The transition state associated with the more favourable stereoisomeric channel: **TS-men** is much more asynchronous than those associated with the other channels. This fact supports the empirical rule that holds for a variety of Diels–Alder cycloadditions that 'for dissymetrically substituted dienophiles, the more asynchronous transition state has the lower energy'.[45–51]

3.2c *Transition vectors and frequencies analysis*: Transition vectors (TVs) analyses allow us to understand the chemical process associated with each transitions structure involved in this 1,3-DC. We have reported in table 6, the imaginary frequencies, the main TVs components and their corresponding geometric parameters for the four transition states. For the two meta-TSs (**TS-men** and **TS-mex**), the dominant TV components are associated with the $C_3–C_5$ (≈0.38) and $O_1–C_4$ (≈0.43) bond distances, which correspond to the two newly σ-bonds formed in these 1,3-DC processes. For the ortho-TSs, the values of the $C_3–C_4$ components (≈0.46–0.51) are larger than for the $O_1–C_5$ ones (≈0.29). It can appear, from these values, the asynchronicity in the bond formation process along this 1,3-DC because the TVs components associated with the $C_3–C_5$ and $O_1–C_5$ bonds are different. Several dihedral angles also participate in the transition vectors. The $H_{a4}–C_4–C_5–H_{a5}$ dihedral angle is associated with the hybridization change that is developing in the C_4 and C_5 centres from sp^2 to sp^3. The $H_{a3}–C_3–N_2–O_1$ dihedral angle shows the sp^2 to sp^3 re-hybridization taking place at the N_2 nitrogen centre along the 1,3-DC reactions. The imaginary frequency values from **TS-men**, **TS-mex**, **TS-oen** and **TS-oex** are 406.9i, 406.6i, 412.4i and 424.1i cm^{-1}, respectively. These values are lower than those for the Diels–Alder cycloadditions (500 cm^{-1}) and indicate that these processes are associated with heavy atom motions and are also related to the earlier TSs.

3.2d *Bond order and charge analysis*: In connection with the structure of the transition states, the bond order

Table 6. Imaginary frequency (cm^{-1}), Hessian unique eigenvalue (au), main components of the transition vector (au) and corresponding geometric parameters (lengths in Angstrom, angles in degree) for the TSs corresponding to the 1,3-DC.

Imaginary frequency eigenvalue	**TS-men**		**TS-mex**	
	406.9i		409.6i	
	−0.01401		−0.01426	
$C_3–C_5$	0.37799	2.286	0.38174	2.276
$O_1–C_4$	0.43420	1.889	0.43277	1.928
H_{a4}, C_4, C_5, H_{a5}	−0.18286	−153.6	0.13904	161.9
H_{a3}, C_3, N_2, O_1	0.22631	−42.3	0.21624	−40.6
Imaginary frequency eigenvalue	**TS-oen**		**TS-oex**	
	412.4i		424.1i	
	−0.01204		−0.01406	
$C_3–C_4$	0.46317	2.036	0.51196	2.036
$O_1–C_5$	0.28721	2.219	0.29544	2.179
H_{a4}, C_4, C_5, H_{a5}	0.08307	160.7	−0.15623	−149.4
H_{a3}, C_3, N_2, O_1	0.20814	−47.3	0.22219	−46.0

Table 7. Charge transfer (NPA qCT), Wiberg bond orders of forming bonds at transition structures and cycloadducts and percentage of their formation at TSs.

	TS-men		**P-men**	**TS-mex**		**P-mex**
NPA qCT (e)	0.09			0.09		
O_1-C_4 (%)	0.4672		0.9040	0.4443		0.9064
		51.68			49.01	
C_3-C_5 (%)	0.3318		0.9689	0.3287		0.9740
		34.24			33.74	
	TS-oen		**P-oen**	**TS-oex**		**P-oex**
NPA qCT (e)	0.09			0.07		
O_1-C_5 (%)	0.2986		0.9322	0.3245		0.9221
		32.03			35.19	
C_3-C_4 (%)	0.4735		0.9843	0.4872		0.9828
		48.10			49.57	

(BO) values are used to analyse of the evolution of bond formation or bond breaking along the reaction pathway. To also understand the molecular mechanism in this study, the Wiberg bond indices[52] have been computed using the NBO population analysis, the results are reported in table 7. General analysis of the bond order values for all the transition structures showed that the cycloaddition process is particularly asynchronous. For the meta-TSs, the values of percentage of forming O_1–C_4 bonds, in the ranges of 51.68–49.01, are greater than those for the forming C_3–C_5 ones (34.24-33.74). For the ortho-TSs, however, the percentage of forming bond O_1–C_5 (35.19–32.03) has lesser values than that of C_3–C_4 bond (49.57–48.10).

A comparative study of the values of activation energies, bond orders and frequencies corroborates the fact that the more asynchronous TSs presents a lower activation barrier and a lower imaginary frequency.[11,51] The charge transfer evaluated by the natural population analysis in terms of the residual charge on the pyrroline-1-oxide fragment, for all the optimized TSs, are listed in table 7. Positive values are indicative of an electron flow from the HOMO/dipole to the LUMO/dipolarophile, in agreement with the electronic chemical potential values, but their magnitudes reveal an almost neutral reaction.

4. Conclusion

In summary, we have checked in the present theoretical study, the regioselectivity and stereoselectivity of the 1,3-dipolar cycloaddition reaction of the cyclic nitrone: pyrroline-1-oxide and methyl crotonate using both frontier molecular orbitals analysis and complete exploration of the potential energy surface at DFT/B3LYP level using the 6-31G* basis set. For this cycloaddition, four reactive pathways have been characterized relative to the endo and exo approaches of the dipolarophile to the dipole along the ortho and meta-regioisomeric pathways. Analysis of FMO energies, electronic chemical potentials and charge transfer at the transition states indicates a normal electron demand character for the reaction. Interaction energies for the global–global and local–global interactions have been investigated revealing a clear preference for the meta-regioselectivity of the cycloaddition process. Geometrical parameter and Wiberg bond indices indicate that the cycloaddition reaction follows a concerted mechanism with asynchronous transition states. General analysis of the bond order values for all the TSs structures showed that the cycloaddition process is asynchronous. This theoretical study shows a clear preference for the meta-regioselectivity of the cycloaddition process in conformity with the experimental findings. This study also demonstrates that B3LYP/6-31G(d) calculations can be used for description of the cycloaddition reaction between the 5-membered cyclic nitrone and an unsymmetrically disubstituted olefin.

Acknowledgement

This work was supported by the Ministry of High Education of Morocco (SCH09/09) project 'Plan d'Urgence' and European PF7 Marie Curie PIRSES-GA-2012-317544 project CAPZEO.

References

1. Padwa A 1984 *1,3-Dipolar cycloaddition chemistry*, vols 1-2 (New York: Wiley Interscience)
2. (a) Padwa A, Tomioka Y and Venkatramanan MK 1987 *Tetrahedron Lett*. **28** 755; (b) Breuer E, Aurich H G and Nielsen 1989 *Nitrones, nitronates and nitroxides* (New York: Wiley); (c) Padwa A 1991 *Comprehensive Organic Synthesis* **4** 1069; (d) Torssell K B G 1998 *Nitrile oxides, nitrones and nitronates in organic synthesis*; (New York: VCH); (e) Gothelf K V and Jørgensen K A 1998 *Chem. Rev*. **98** 863; (f) Bortolini O, Mulani I,

De Nin A, Maiuolo L, Nard M, Russo B and Avnet S 2011 *Tetrahedron* **67** 563; (g) Majumder S and Bhuyan P J 2012 *Tetrahedron Lett*. **53** 762
3. (a) Minter A R, Brennan B B and Mapp A K 2004 *J. Am. Chem. Soc*. **126** 10504; (b) Palmer G C, Ordy M J, Simmons R D, Strand J C, Radov L A, Mullen G, Kinsolving C R, Mitchell J T and Alle S D 1989 *Antimicrob. Agents Chemother*. **33** 895
4. Ding P, Miller M, Chen Y, Helquist P, Oliver A J and Wiest O 2004 *Org. Lett*. **6** 1805
5. Wess G, Kramer W, Schuber G, Enhsen A, Baringhaus K H, Globmik H, Müller S, Bock K, Klein H, John M, Neckermann G and Hoffmann A 1993 *Tetrahedron Lett*. **34** 819
6. Padwa A and Pearson W H 2002 *Synthetic applications of 1,3-dipolar cycloaddition chemistry toward heterocycles and natural products* (New York: Wiley & Sons)
7. Marakchi K, Kabbaj O K and Komiha N 2002 *J. Fluorine Chem*. **114** 81
8. Marakchi K, Kabbaj O K, Komiha N, Jalal R and Esseffar M 2003 *J. Mol. Struct. (Theochem)* **620** 271
9. Liu J, Niwayama S, You Y and Houk K N 1998 *J. Org. Chem.* **63** 1064
10. Cossó F P, Marao I, Jiao H and Schleyer P V R 1999 *J. Am. Chem. Soc.* **121** 6737
11. Cadra V, Portoleś R, Murga J, Uriel S, Marco J A, Domingo L R and Zaragoza R J 2000 *J. Org. Chem.* **65** 7000
12. Domingo L R 2000 *Eur. J. Org. Chem.* 2265
13. Nacereddine A K, Yahia W, Bouacha S and Djerourou A 2010 *Tetrahedron Lett.* **51** 2617
14. Stecko S, Michel C, Milet A, Pérez S and Chmielewski M 2008 *Tetrahedron: Asymmetry* **19** 2140
15. Acharjee N and Banerji A 2011 *Comput. Theor. Chem.* **967** 50
16. Asrof Ali Sk, Khan J H, Wazeer M I M and Perzanowski H P 1989 *Tetrahedron* **45** 5979
17. Frisch M J *et al. Gaussian 03, Revision B.04 Gaussian*: Pittsburgh PA 2003
18. Becke A D J 1988 *Chem. Phys.* **38** 3098
19. Lee C Yang and W Parr R G 1988 *Phys. Rev.* **B37** 785
20. Hehre W J, Radom L, Schleyer P R and Pople J A 1986 *Ab initio molecular orbital theory* (New York: Wiley)
21. Gonzalez C and Schlegel H B 1989 *J. Chem. Phys.* **90** 2154
22. Gonzalez C and Schlegel H B 1990 *J. Phys. Chem.* **94** 5523
23. (a) Reed A E, Curtiss L A and Weinhold F 1988 *Chem. Rev.* **88** 899; (b) Reed A E Weinstock R B and Weinhold F 1985 *J. Chem. Phys.* **83** 735
24. Parr R G and Yang W 1989 *Density functional theory of atoms and molecules* (New York: Oxford University)
25. (a) Domingo L R, Chamorro E and Pérez P J 2088 *J. Org. Chem.* **73** 4615; (b) Domingo L R and Picher M T 2004 *Tetrahedron* **60** 5053
26. Domingo L R, Aurell M J, Pérez P and Contreras R 2002 *J. Phys. Chem.* **A106** 6871
27. Geerlings P, De Prof F and Langenaeker W 2003 *Chem. Rev.* **103** 1793
28. Pérez P, Domingo L R, Duque-Norna M and Chamorro E 2009 *J. Mol. Struct. (Theochem)* **895** 86
29. Yang W and Mortier W J 1986 *J. Am. Chem. Soc.* **108** 5708
30. Tomasi J and Persico M 1994 *Chem. Rev.* **94** 2027
31. Kumar Das T, Salampuria S and Banerjee M 2010 *J. Mol. Struct. (Theochem)* **959** 22
32. Ohgaki E, Motoyoshiya J, Narita S, Kakurai T, Hayashi S and Hirakawa K 1990 *J. Chem. Soc. Perkin Trans.* **1** 3109
33. Aso M, Ojida A, Yang G, Cha O, Osawa E and Kanematsu K 1993 *J. Org. Chem.* **58** 3960
34. Steck S, Michel C, Milet A, Perez S and Chmielewski M 2008 *Tetrahedron: Asymmetry* **19** 1660
35. Wei D, Zhu Y, Zhang C, Sun D, Zhang W and Tang M 2011 *J. Mol. Catal. A: Chem.* **334** 108
36. Marakchi K, Kabbaj O K, Komiha N and Chraibi M 2001 *J. Fluorine Chem.* **109** 163
37. Marakchi K, Kabbaj O K, Komiha N and Abou El Makarim H 2010 *Phys. Chem. News* **52** 128
38. Naji N, Marakchi K, Kabbaj O K, Komiha N, Chraibi M, Joffre J and Soufiaoui M 1999 *J. Fluorine Chem.* **94** 127
39. Sheng Y H, Fang D C, Wuc Y D, Fub X Y and Jianga Y 1999 *J. Mol. Struct. (Theochem)* **467** 31
40. Sustman R and Sicking W 1987 *Chem. Ber.* **120** 1653
41. Sustman R and Sicking W 1987 *Chem. Ber.* **120** 1471
42. Houk K N 1975 *Acc. Chem. Res.* **8** 361
43. Merino P, Revuelta J, Tejero T, Chiacchio U, Rescifina A and Romeo G 2003 *Tetrahedron* **59** 3581
44. Pérez P, Domingo L R, Aurell M J and Conteras R 2003 *Tetrahedron* **59** 3117
45. (a) Domingo L R, Aurell M J, Pérez P and Contreras R 2002 *Tetrahedron* **58** 4417; (b) Domingo L R, Asensio A and Arroyo P 2002 *J. Phys. Org. Chem.* **15** 660; (c) Domingo L R, Arno M, Contreras R and Pérez P 2002 *J. Phys. Chem. A* **106** 952; (d) Domingo LR 2002 *Tetrahedron* **58** 3765; (e) Domingo L R, Aurell M J, Pérez P and Contreras R 2003 *J. Org. Chem.* **68** 3884; (f) Domingo L R and Andres J 2003 *J. Org. Chem.* **68** 8662; (g) Jasiński R, Koifman O I and Barański A 2011 *Mendeleev Commun.* **21** 262; (h) Domingo L R, Pérez P and Sáez J A 2004 *Tetrahedron* **60** 11503
46. Simkin B Y and Sheikhet I I 1995 *Quantum chemical and statistical theory of solutions. A computational approach* (London: Ellis Horwood Ltd.)
47. (a) Cances M T, Mennunci V and Tomasi J 1997 *J. Chem. Phys.* **107** 3032; (b) Cossi M, Barone V, Cammi R and Tomasi J 1996 *J. Chem. Phys. Lett.* **255** 327; (c) Barone V, Cossi M and Tomasi J 1998 *J. Comput. Chem.* **19** 404
48. Mendez F, Tamariz J and Geerlings P 1998 *J. Phys. Chem.* **A102** 6292
49. Froese R D J, Organ M G, Goddard J D, Stack T D P and Trost B M 1995 *J. Am. Chem. Soc.* **117** 10931
50. Garcia J I, Martinez-Merino V, Mayoral J A and Salvatella L 1998 *J. Am. Chem. Soc*. **120** 2415
51. Domingo L R 1999 *J. Org. Chem.* **64** 3922
52. Wiberg K B 1968 *Tetrahedron* **24** 1083